JACS
JOURNAL OF THE AMERICAN CHEMICAL SOCIETY

COMMUNICATION

pubs.acs.org/JACS

Selective Dispersion of Single-Walled Carbon Nanotubes with Specific Chiral Indices by Poly(*N*-decyl-2,7-carbazole)

Fabien A. Lemasson,[†] Timo Strunk,[†] Peter Gerstel,[⊥] Frank Hennrich,[†] Sergei Lebedkin,[†] Christopher Barner-Kowollik,[⊥] Wolfgang Wenzel,*[,†,§] Manfred M. Kappes,*[,†,§,∥] and Marcel Mayor*[,†,§,‡]

[†]Institut für Nanotechnologie, Karlsruher Institut für Technologie, 76021 Karlsruhe, Germany,

[⊥]Institut für Technische Chemie und Polymerchemie, Karlsruher Institut für Technologie, 76128 Karlsruhe, Germany

[§]DFG Center for Functional Nanostructures, 76028 Karlsruhe, Germany

[∥]Institut für Physikalische Chemie, Karlsruher Institut für Technologie, 76128 Karlsruhe, Germany

[‡]Department of Chemistry, University of Basel, 4056 Basel, Switzerland

Supporting Information

ABSTRACT: Physico-chemical methods to sort single-walled carbon nanotubes (SWNTs) by chiral index are presently lacking but are required for in-depth experimental analysis and also for potential future applications of specific species. Here we report the unexpected selectivity of poly(*N*-decyl-2,7-carbazole) to almost exclusively disperse semiconducting SWNTs with differences of their chiral indices $(n - m) \geq 2$ in toluene. The observed selectivity complements perfectly the dispersing features of the fluorene analogue poly(9,9-dialkyl-2,7-fluorene), which disperses semiconducting SWNTs with $(n - m) \leq 2$ in toluene. The dispersed samples are further purified by density gradient centrifugation and analyzed by photoluminescence excitation spectroscopy. All-atom molecular modeling with decamer model compounds of the polymers and (10,2) and (7,6) SWNTs suggests differences in the $\pi-\pi$ stacking interaction as origin of the selectivity. We observe energetically favored complexes between the (10,2) SWNT and the carbazole decamer and between the (7,6) SWNT and the fluorene decamer, respectively. These findings demonstrate that subtle structural changes of polymers lead to selective solvation of different families of carbon nanotubes. Furthermore, chemical screening of closely related polymers may pave the way toward simple, low-cost, and index-specific isolation of SWNTs.

Due to their unique physical and mechanical properties, single-walled carbon nanotubes (SWNTs) have attracted much research attention, and their applications range over micro-/opto-electronics,[1] high strength fibers, and nanocomposites.[2] The physical properties of SWNTs are dictated by their chiral index (n,m) and length. Despite numerous methods for producing these materials,[3] none of them are selective; i.e., a mixture of SWNTs in terms of (n,m) indices and metallicity is obtained. Thus, many applications require the products to be sort by length, electrical behavior, and/or diameter,[4] so that post-processing of pristine SWNTs concentrates many efforts.[3−9] Covalent and non-covalent functionalizations are the main two approaches. The first one alters the SWNT's intrinsic properties, which is obviously not acceptable for applications in electronics. However, in the latter approach, SWNTs interact with molecules via van der Waals or $\pi-\pi$ interactions, thus keeping the sp^2 hybridization of their C-atoms unchanged, which only slightly alters the electronic properties.[4,5,10]

The first step in any purification or sorting attempt is the debundling of the parent aggregates of carbon material in order to isolate individual SWNTs. Sonication-assisted dispersion of the raw material in a suitable solvent results ideally in a large fraction of individual debundled nanotubes. Such dispersions of nanotubes are usually stabilized by water-soluble polymers[11] or surfactants in water or by polymers in organic solvents.[5−10,12] Polymers comprising aromatic subunits either in their backbones or in their side chains displayed very good dispersing properties. Particularly appealing features were found for polymers consisting of backbones comprising 9,9-dialkyl-2,7-fluorene subunits, which displayed unexpected selectivity for semiconducting tubes. Furthermore, mainly semiconducting tubes with differences in indices $(n - m) = 1$ or 2 and thus large chiral angles Θ were dispersed by these polymers. Variation of the polymer backbone by different aryl subunits interlinking the fluorenes enabled further fine-tuning of the observed selectivities.[5−9]

Inspired by these results, we became interested in the carbazole polymer **1** as a structural proxy of the fluorene polymer **2**, but with only one "dissolving" alkyl chain per polymer unit. Moreover, the N-bridging atom is planar, the C-bridging atom of fluorene **2** being tetragonal. Here we report that polymer **1** is also selective in dispersing semiconducting SWNTs but complements the behavior of the fluorene analogue **2**, in that exclusively lower chiral angles can be accessed.

N-Alkylated polycarbazoles were already reported,[13] and the synthesis providing the polymer **1** is displayed in Scheme 1.[14]

The nanotube-dispersing features of the polymers **1** and **2** were analyzed by treating ∼1 mg of as-prepared HiPco SWNTs together with ∼50 mg of the polymer under investigation in ∼15 mL of toluene with a titanium sonotrode for 2 h.[14] Larger agglomerates were removed by gel filtration, and density gradient centrifugation (DGC) was applied as purification method in order to collect the entirety of polymer-stabilized dispersions.[14] Indeed,

Received: April 19, 2010
Published: December 20, 2010

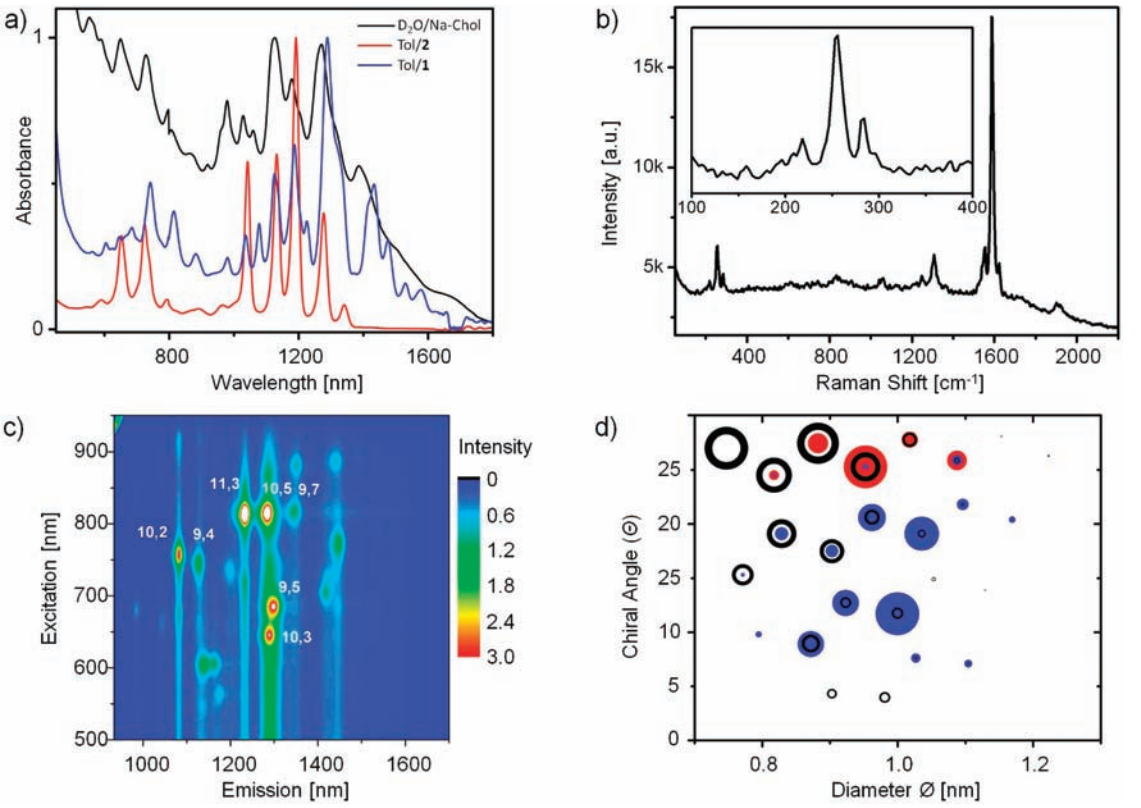

Figure 1. (a) Absorption spectra of the HiPco SWNTs in D_2O/Na-cholate (black) and of the SWNT/polymer dispersions in toluene (Tol/**1**, blue; Tol/**2**, red).[14] (b) Raman spectrum of Tol/**1** dispersion recorded on dried sample. (c) PLE map (color-coded emission intensity in arbitrary units vs excitation and emission wavelengths) of Tol/**1** dispersion after DGC.[10] (d) Θ/Ø map from extracted PLE intensities transformed into normalized area of cycles (D_2O/Na-cholate in black, Tol/**1** in blue, and Tol/**2** in red).[14]

Scheme 1. Structures of the Polymers 1 and 2 Together with the Synthesis of 1 and Its Precursors 4 and 5[a]

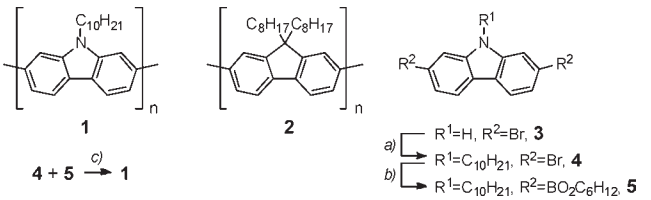

[a] Conditions: (a) K_2CO_3, $Br(CH_2)_9CH_3$, DMF, rt, 71%; (b) $-(BO_2C_6H_{12})_2$, $Pd(dppf)Cl_2$, DMF, 85 °C, 61%; (c) $Pd(PPh_3)_4$, $C_6H_5CH_3$, 1 M Na_2CO_3, 85 °C, 76%.

polymer/SWNTs complexes having a density higher than that of toluene would be lost by applying normal centrifugation.

Already the absorption spectra of the filtered dispersions indicated that different fractions of the parent mixture of SWNTs were dispersed by the polycarbazole **1** compared with the polyfluorene **2** (Figure 1a). The absorption bands of metallic tubes, which appear between 300 and 600 nm for HiPco SWNTs (thus overlaying some semiconducting tubes), are clearly missing in the case of suspensions prepared from polymers **1** and **2**. Almost all signals present in the absorption spectra were assigned.[14] Together with a good signal-to-noise ratio, these show that polymer **1** is selectively dispersing semiconducting tubes. This feature is also observed in the Raman spectra of SWNT/polycarbazole **1** (Figure 1b).[14] For unsorted HiPco SWNTs, radial breathing mode (RBM) frequencies are obtained between 180 and 300 cm^{-1}. The metallic tubes show up between ~180 and ~230 cm^{-1}, whereas semiconducting tubes appear between ~220 and ~300 cm^{-1}.[15] In the Raman spectrum taken from tubes wrapped by polycarbazole **1**, the *metallic* RBM region is almost completely suppressed. The *semiconducting* RBM frequencies can be assigned to tubes that are found in the photoluminescence excitation (PLE) maps and are accessible through excitation with 632.8 nm: (12,2), (9,5), (10,3), (8,4), and (8,3), with 227, 245, 256, 280, and 296 cm^{-1}, respectively.[14]

The polymer stabilized dispersions were further analyzed by PLE spectroscopy. The PLE map of the **1**-stabilized dispersion after DGC is displayed in Figure 1c, and in spite of a small hypsochromic shift,[14] it allows us to assign the (n,m) indices of the SWNTs.[16−18] Interestingly, the fraction stabilized by **1** consists almost exclusively of SWNTs with $(n - m) \geq 2$ and is thus complementary to the fraction stabilized by **2**.

The chiral angles (Θ) vs nanotube diameter (Ø) map displayed in Figure 1d nicely visualizes the complementary fractions wrapped by each of the polymers. The intensity of the PLE signal of each tube observed by PLE spectroscopy of the dispersion was translated into the size of the circle in the Θ/Ø map. The composition of the SWNT raw material is represented by the Na-cholate-stabilized dispersion in D_2O (black circles in Figure 1d), which is mainly a mixture of about 20−30 different metallic and semiconducting types of carbon nanotubes. The SWNTs stabilized by the polycarbazole **1** are displayed as blue circles, while the ones stabilized by polyfluorene **2** are displayed as red circles

dx.doi.org/10.1021/ja105722u | J. Am. Chem. Soc. 2011, 133, 652–655

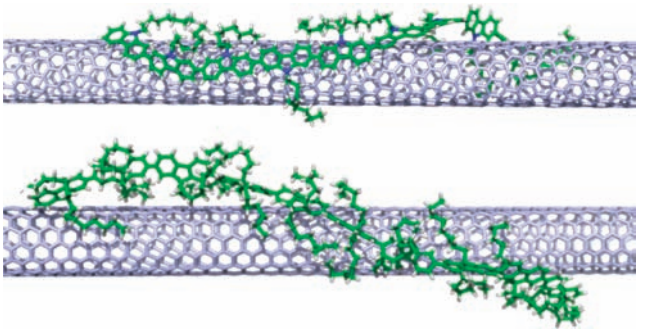

Figure 2. Minimum energy conformations of the decamer/(n,m) tube obtained by molecular dynamics simulation. Top: carbazole decamer **1** and a (10,2) nanotube. Bottom: fluorene decamer **2** and the (7,6) nanotube.

in Figure 1d. As the products of the absorption cross section (per mol of carbon) and PLE quantum yield at E_{22} excitation appear to depend only moderately on the nanotube structures,[19] the Θ/Ø map also provides a quantitative estimate of the composition of the dispersions. Obviously, both polymers **1** and **2** selectively disperse semiconducting nanotubes in a comparable diameter range between 0.8 and 1.1 nm but with different chiral angles Θ. Their selectivity toward a small group of SWNTs points toward specific interactions between the polymers and SWNTs.[20]

In order to investigate this hypothesis theoretically, atomistic simulations were performed.[14] The SWNTs with chiral indices (7,6) and (10,2) were chosen as representative model systems because they have comparable diameters but were each preferentially dispersed by only one of the two polymers. Starting from conformations with well-separated decamers of both polymer structures and nanotubes, all four decamer/nanotube combinations were initially optimized by four independent basin hopping simulations to obtain the energetically best starting conformation for long annealing simulations for each polymer/tube combination.[21−24]

We immediately observed that the fluorene decamer representative of polymer **2** showed no tendency to wrap around the (10,2) nanotube, lying essentially flat on the tube. This qualitative result was obtained in all four independent simulations. In contrast, some wrapping of the fluorene compound was observed for the (7,6) tube, as illustrated in the bottom part of Figure 2. The energies of this complex were significantly lower than for the (10,2) tube (red symbols in Figure 3). A more subtle situation was observed for the carbazole decamer as model compound for polymer **1**, in which a close alignment of the rings of the polymer and the tubes was observed. Here we observed the complexes formed with the (10,2) tube (Figure 2, top) to be energetically favored compared to the ones formed with the (7,6) tubes (Figure 3, blue symbols). Because the energy model incorporates a short-range term for the $\pi-\pi$ interactions between the aromatic carbons and the polymer models and the CNTs, the binding energy is dominated by the number of aromatic C−C contacts in the complex. The number of such contacts is constrained by the geometry of the molecule, which has only one free backbone dihedral per unit and steric repulsion between the side chain atoms and the CNT. The results of the fluorene−(10,2) simulations indicate that only the "trivial" solution (all backbone dihedrals straight) is possible for this system. When the radius of the tube changes or the side-chain constraints simplify by removing one side chain, other solutions for the backbone dihedrals become feasible. The chiral index of the tube will then determine how many favorable aromatic contacts become

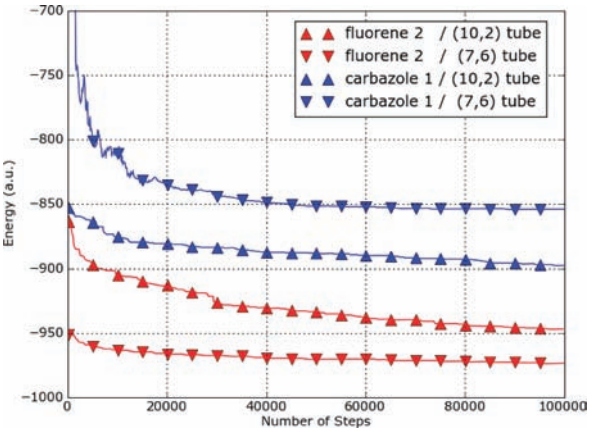

Figure 3. Energies of the final simulated annealing runs[14] (only first 100 000 are steps shown) for the binding energy of the decamer/CNT complexes for the fluorene/carbazole (red/blue symbols) and the (10,2) and (7,6) tubes (triangles up/down, respectively), demonstrating a reversal of the relative binding propensity of the polymer models with the different CNTs. Note that the energy scale of absolute binding energies is arbitrary because the polymer desolvation energy is not taken into account.

possible, which obviously depends on many nontrivial geometrical constraints. The increased tendency of the carbazole decamer to wrap around both types of tubes thus results from an increased $\pi-\pi$ interaction made possible by the reduced steric requirements of a single alkyl chain at the bridging atom.

In conclusion, the ability of poly(*N*-decyl-2,7-carbazole) **1** to disperse SWNTs was investigated. An unexpected selectivity toward semiconducting nanotubes with $(n - m) \geq 2$ was found which is complementary to the semiconducting SWNTs which are preferentially dispersed by the fluorene analogue **2**. The compositions of the dispersed fractions were analyzed by PLE spectroscopy and were displayed by a Θ/Ø map. The preferences of both polymers for particular chiral angles were also found in molecular dynamic simulations with decamers as model compounds for the polymers and (10,2) and (7,6) SWNTs.

Currently, we are varying the polymers structure in order to further investigate the nature and the selectivity of the polymer nanotube interactions.

■ ASSOCIATED CONTENT

Ⓢ Supporting Information. Synthetic protocols and analytical data of the polymer **1** and its precursors **3**−**5**; experimental details concerning the dispersion, filtration, and DGC of the SWNTs; tables of all identified SWNTs; a table of spectral shifts caused by the dispersing agents; a graphene lattice diagram; and details about the molecular dynamic and absorption spectra simulations. This material is available free of charge via the Internet at http://pubs.acs.org.

■ AUTHOR INFORMATION

Corresponding Author

wolfgang.wenzel@kit.edu; manfred.kappes@kit.edu; marcel.mayor@unibas.ch

■ ACKNOWLEDGMENT

We gratefully acknowledge the support of the KIT, the University of Basel, and the FP7 project MINOTOR.

REFERENCES

(1) Ajayan, P. M. *Chem. Rev.* **1999,** *99,* 1787–1799. Opatkiewicz, J.; LeMieux, M. C.; Bao, Z *ACS Nano* **2010,** *4,* 2975–2978.

(2) Moniruzzaman, M.; Winey, K. I. *Macromolecules* **2006,** *39,* 5194–5205.

(3) (a) Reich, S.; Thomsen, C.; Maultzsch, J. *Carbon Nanotubes: Basic Concepts and Physical Properties*; Wiley-VCH: Weinheim, 2004. (b) O'Connell, M. J. *Carbon Nanotubes: Properties and Applications*: CRC Press Taylor & Francis Group: Boca Raton, FL, 2006.

(4) Martel, R. *ACS Nano* **2008,** *2,* 2195–2199.

(5) Nish, A.; Hwang, J.-Y.; Doig, J.; Nicholas, R. J. *Nature Nanotechnol.* **2007,** *2,* 640–646.

(6) Hwang, J.-Y.; Nish, A.; Doig, J.; Douven, S.; Chen, C.-W.; Chen, L.-C.; Nicholas, R. J. *J. Am. Chem. Soc.* **2008,** *130,* 3543–3553.

(7) Chen, F.; Wang, B.; Chen, Y.; Li, L.-J. *Nano Lett.* **2007,** *7,* 3013–3017.

(8) Cheng, F.; Imin, P.; Maunders, C.; Botton, G.; Adronov, A. *Macromolecules* **2008,** *41,* 2304–2308.

(9) Stürzl, N.; Hennrich, F.; Lebedkin, S.; Kappes, M. M. *J. Phys. Chem. C* **2009,** *113,* 14628–14632.

(10) Moore, V. C.; Strano, M. S.; Haroz, E. H.; Hauge, R. H.; Smalley, R. E. *Nano Lett.* **2003,** *3,* 1379–1382.

(11) Kang, Y. K.; Lee, O.-S.; Deria, P.; Kim, S. H.; Park, T.-H.; Bonnell, D. A.; Saven, J. G.; Therien, M. J. *Nano Lett.* **2009,** *9,* 1414–1418.

(12) Chen, J.; Liu, H.; Weimer, W. A.; Halls, M. D.; Waldeck, D. H.; Walker, G. C. *J. Am. Chem. Soc.* **2002,** *124,* 9034–9035.

(13) (a) Bloin, N.; Leclerc, M. *Acc. Chem. Res.* **2008,** *41,* 1110–1119. (b) Boudreault, P.-L. T.; Blouin, N.; Leclerc, M. *Adv. Polym. Sci.* **2008,** *212,* 99–124. (c) Morin, J.-F.; Leclerc, M. *Macromolecules* **2001,** *34,* 4680–4682.

(14) Details are provided in the Supporting Information.

(15) Hennrich, F.; Krupke, R.; Kappes, M. M.; v. Löhneysen, H. *J. Nanosci. Nanotechnol.* **2005,** *5,* 1166–1171.

(16) Bachilo, S. M.; Strano, M. S.; Kittrell, C.; Hauge, R. H.; Smalley, R. E.; Weisman, R. B. *Science* **2002,** *298,* 2361–2366.

(17) Weisman, R. B.; Bachilo, S. M. *Nano Lett.* **2003,** *3,* 1235–1238.

(18) Lebedkin, S.; Hennrich, F.; Kiowski, O.; Kappes, M. M. *Phys. Rev. B* **2008,** *77,* 165429.

(19) Tsyboulski, D.; Rocha, J.-D. R.; Bachilo, S. M.; Cognet, L.; Weisman, R. B. *Nano Lett.* **2007,** *7,* 3080–3085.

(20) in het Panhuis, M.; Maiti, A.; Dalton, A. B.; van den Noort, A.; Coleman, J. N.; McCarthy, B.; Blau, W. J. *J. Phys. Chem. B* **2003,** *107,* 478–482.

(21) Bogdan, T. V.; Wales, D. J.; Calvo, F. *J. Chem. Phys.* **2006,** *124,* 044102.

(22) Chakravarty, C.; Hinde, R. J.; Leitner, D. M.; Wales, D. J. *Phys. Rev. E* **1997,** *56,* 363–377.

(23) Verma, A.; Schug, A.; Lee, K. H.; Wenzel, W. *J. Chem. Phys.* **2006,** *124,* 044515.

(24) Schug, A.; Herges, T.; Verma, A.; Lee, K. H.; Wenzel, W. *ChemPhysChem* **2005,** *6,* 2640–2646.